

SUPPORTING INFORMATION

Transmembrane Ion Transport through Self-assembling α,γ -Peptide Nanotubes

Rebeca García-Fandiño, Manuel Amorín,* Luis Castedo, and Juan R. Granja*

*Departamento de Química Orgánica y Unidad Asociada al C.S.I.C. Centro Singular de Investigación en
Química Biológica y Materiales Moleculares (CIQUS), Universidad de Santiago de Compostela, 15782
Santiago de Compostela, Spain*

Supporting Information

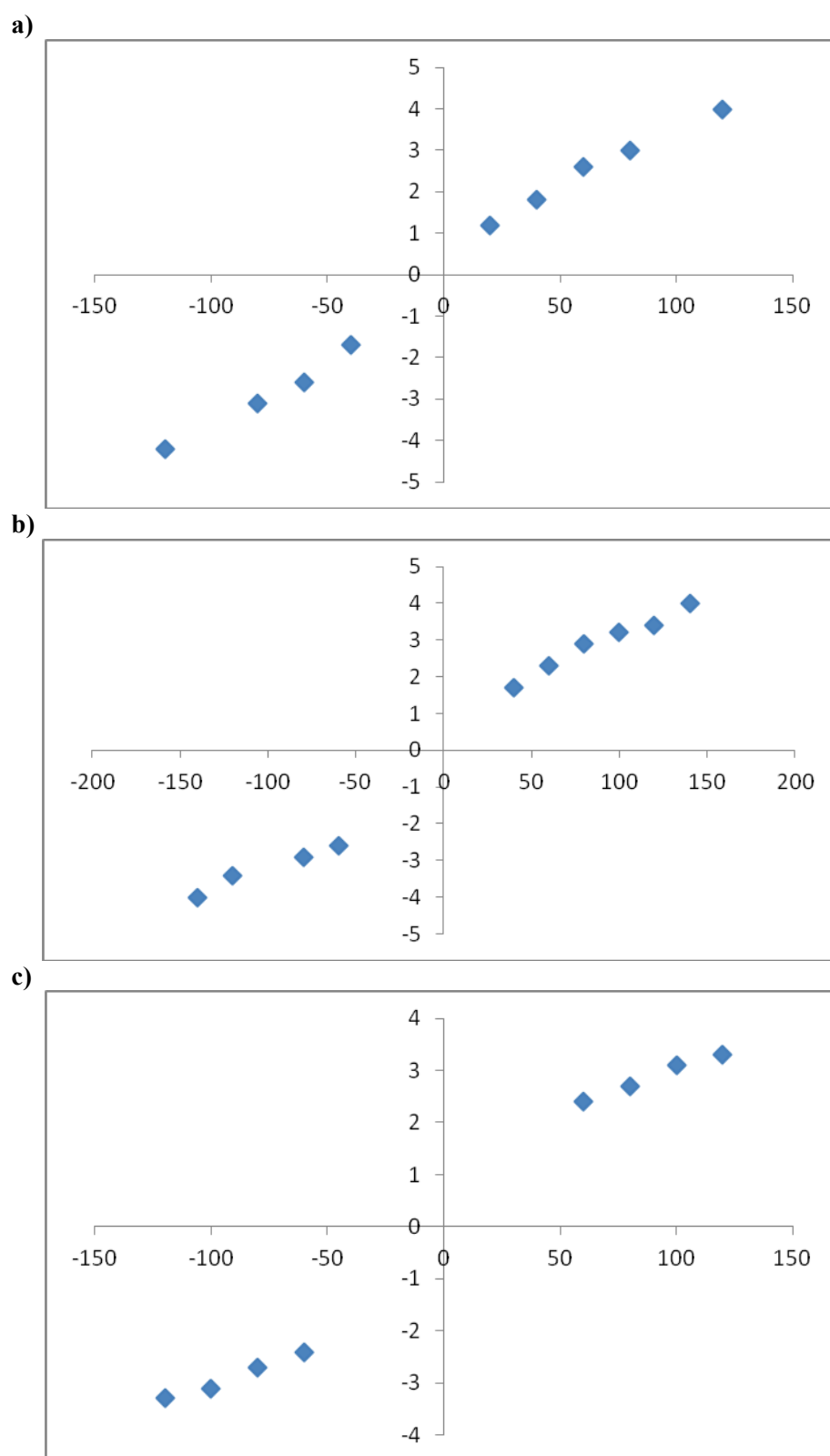


Fig. 1SI Current vs voltage observable for **CP2** transmembrane channels in the presence of a) CsCl (0.5 mM), b) KCl (0.5 mM) and c) NaCl (0.5 mM).

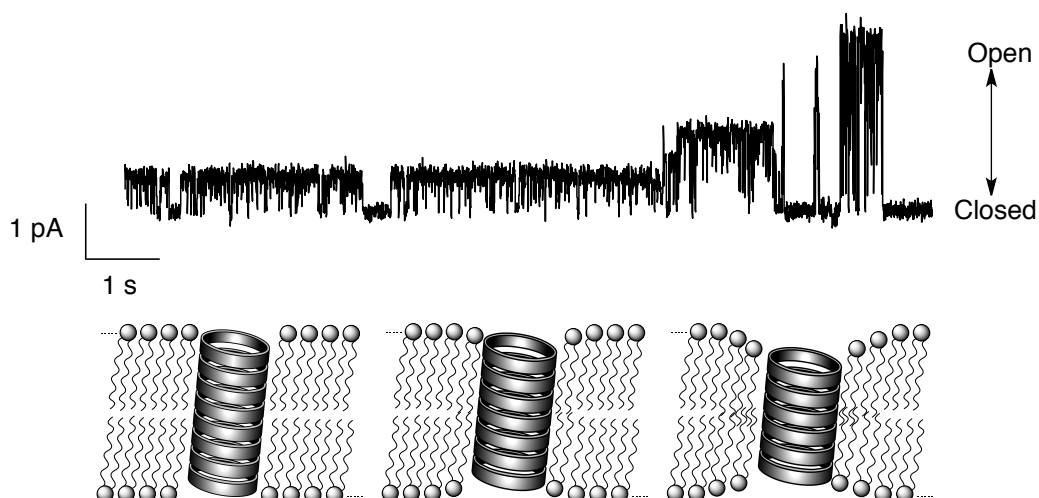


Fig. 2SI Ion channels activity at different conducting states. KCl 0.5 mM (10 mM MOPS. DPPC). 12 seconds of recording with three levels of 0.6 pA, 1.3 pA y 2.9 pA (+80 mV). Filter at 100Hz (Gaussian Filter).

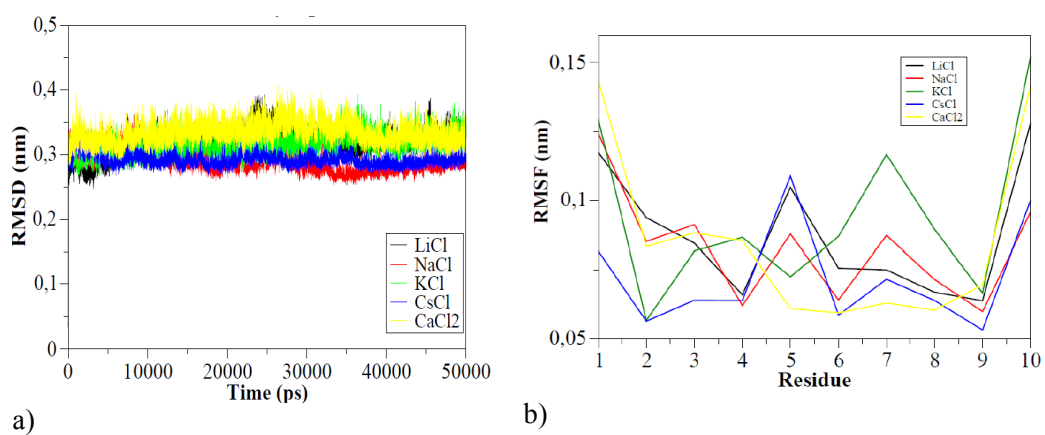


Fig. 3SI a) RMSD and b) RMSF of the SCPN in different salt concentrations.

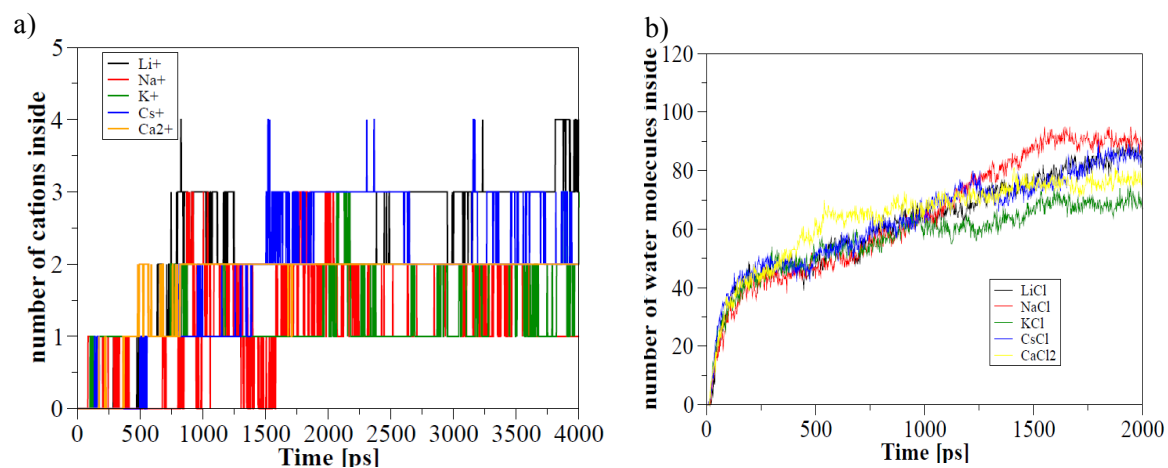


Fig. 4SI Time filling of the nanotubes with ions a) and water b) at different salt concentrations (0.5M LiCl, NaCl, KCl, CsCl and CaCl₂).

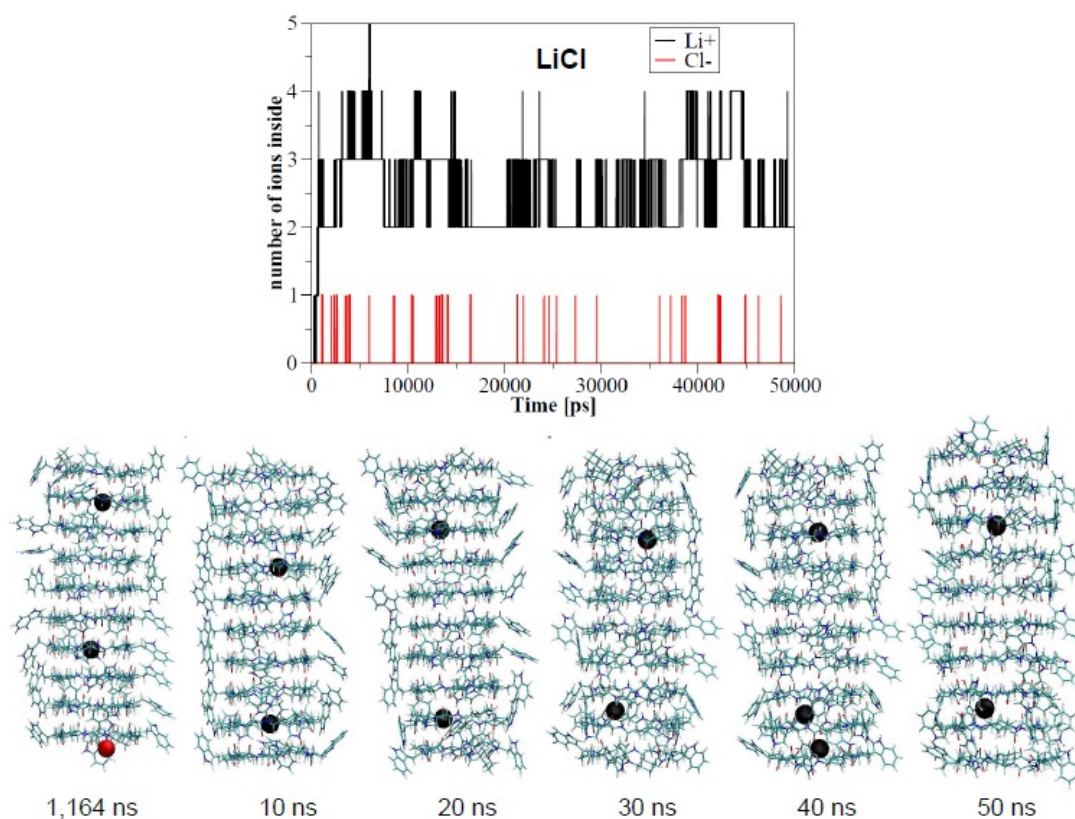


Fig. 5SI Different snapshots at different times of the system simulated in LiCl 0.5 M. Lipids, waters and external ions were removed for clarity.

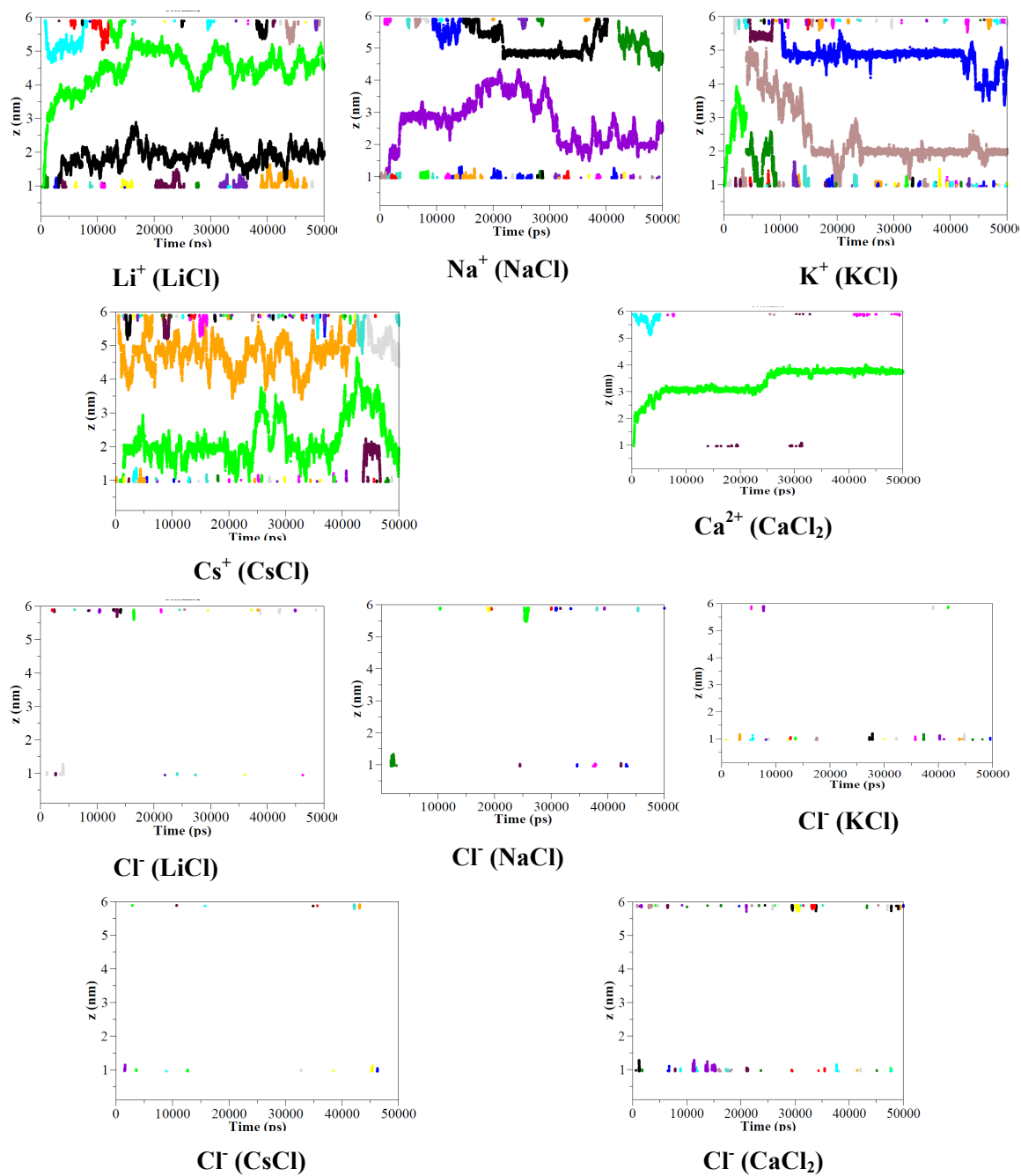


Fig. 6SI Z coordinate for the ions inside the nanotube along the 50 ns trajectory for the different salt concentrations studied.

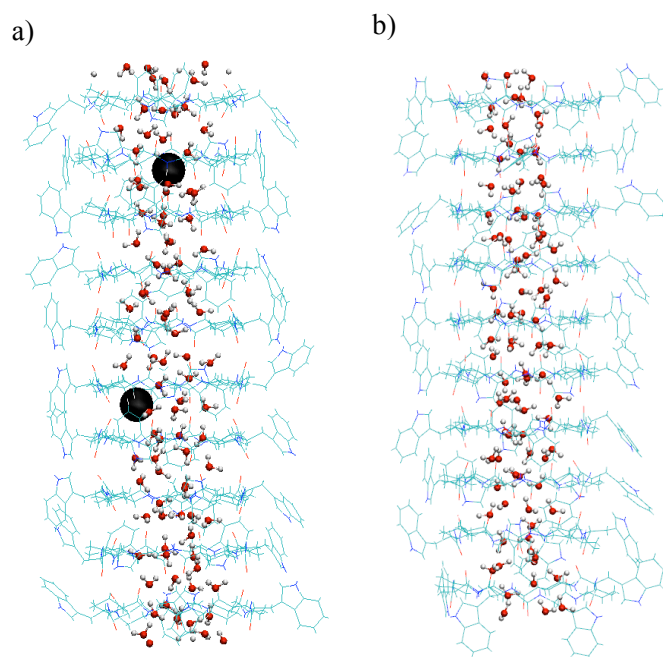


Fig. 7SI a) Snapshot from the simulation of the system in LiCl 0.5M and b) in pure water, pointing out the structure of the internal water and ions. Lipids and external water and ions were removed for clarity.

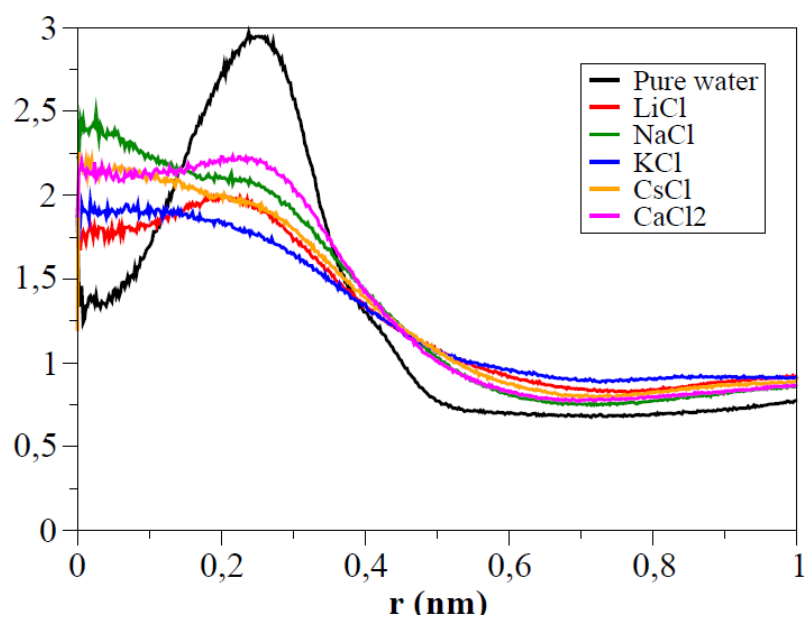


Fig. 8SI Radial distributions of water inside the nanotubes solvated with pure water or with different salt concentrations.

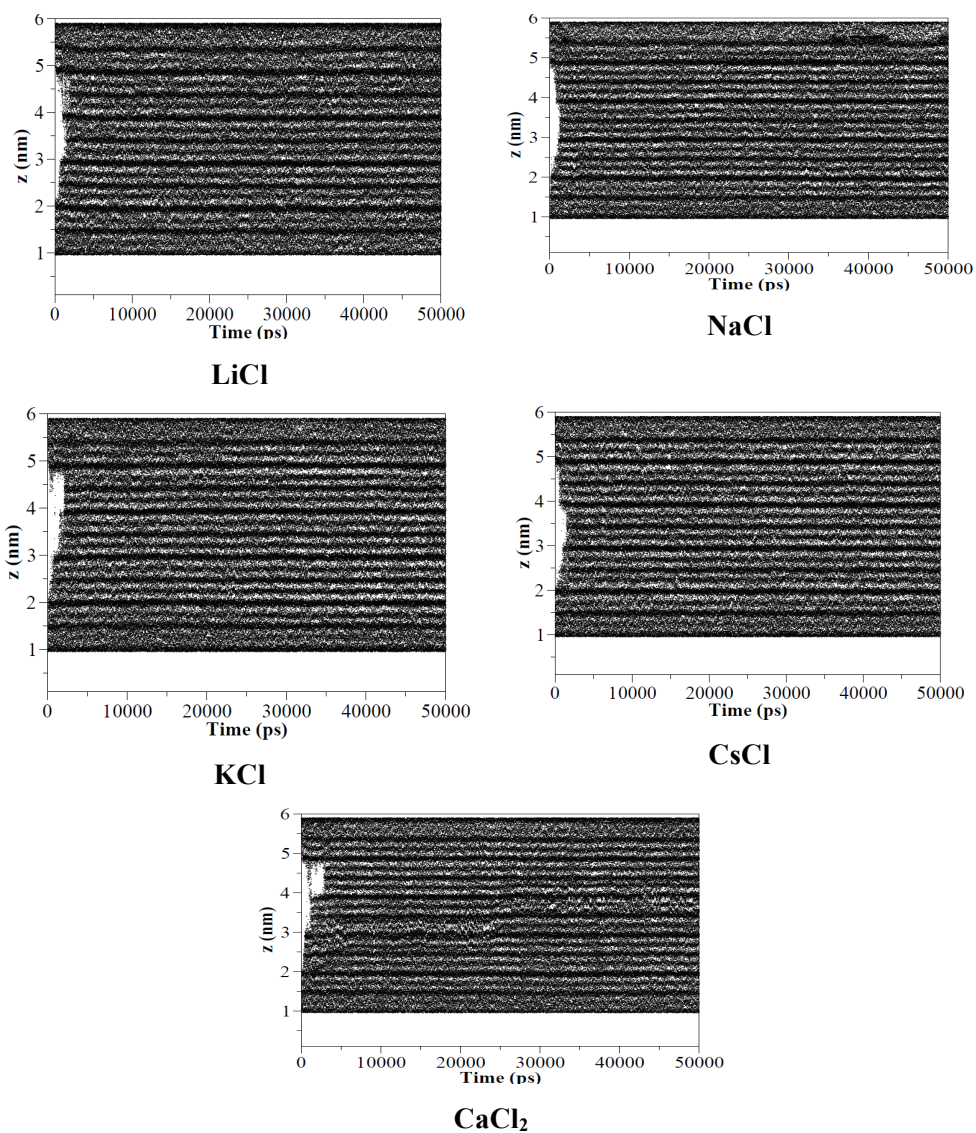


Fig. 9SI Z-coordinate of the internal waters populating the inner cavity of the nanotube in the simulations at different salt concentrations.

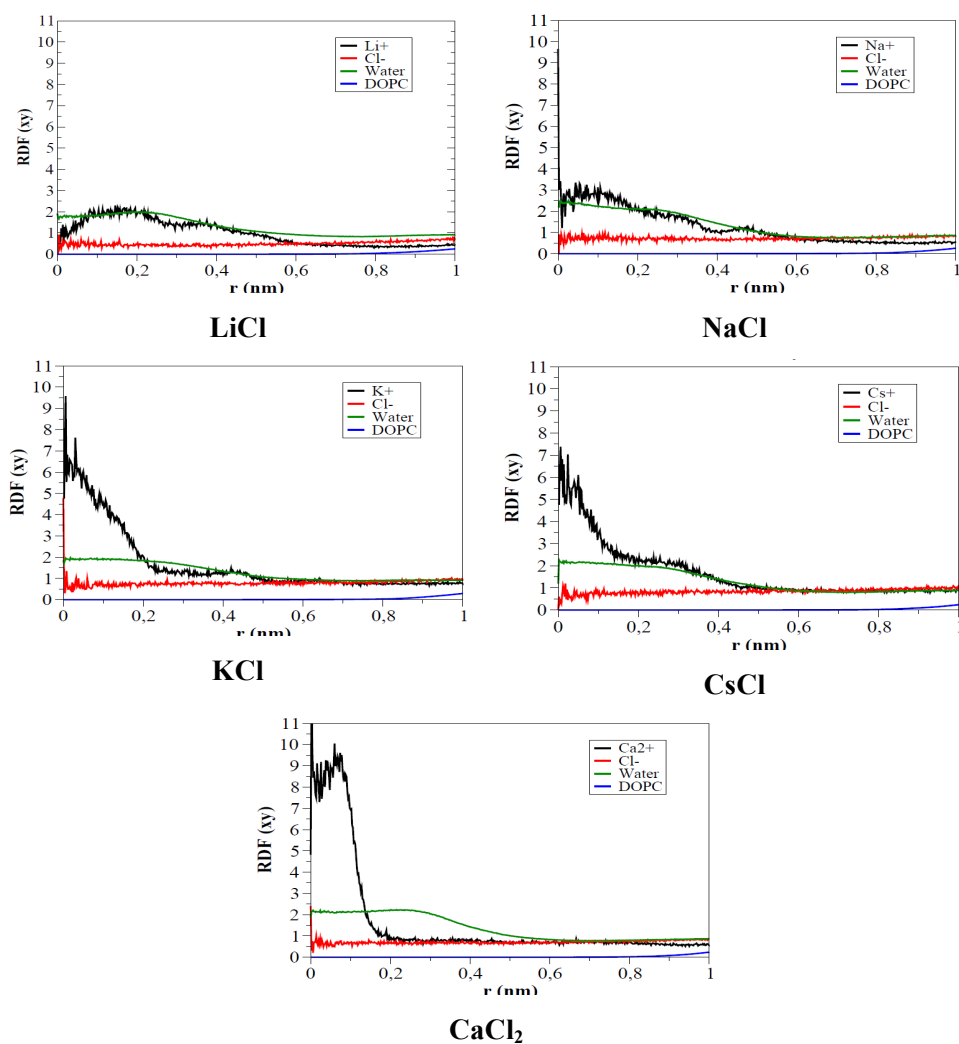


Fig. 10SI Radial distributions of cations (black), Cl⁻ ions (red), water (green), and lipids (blue) inside the nanotubes simulated in different salt concentrations. NOTE: The effective radius of the nanotube is 0.33 nm (HOLE),¹ however taking into account the side chains of the cyclic peptides, the nanotube has a radial length of about 1.4 nm.

¹ O. S. Smart, J. G. Neduvilil, X. Wang, B. A. Wallace, M. S. P. Sansom, *J Mol Graph* **1996**, *14*, 354-360.

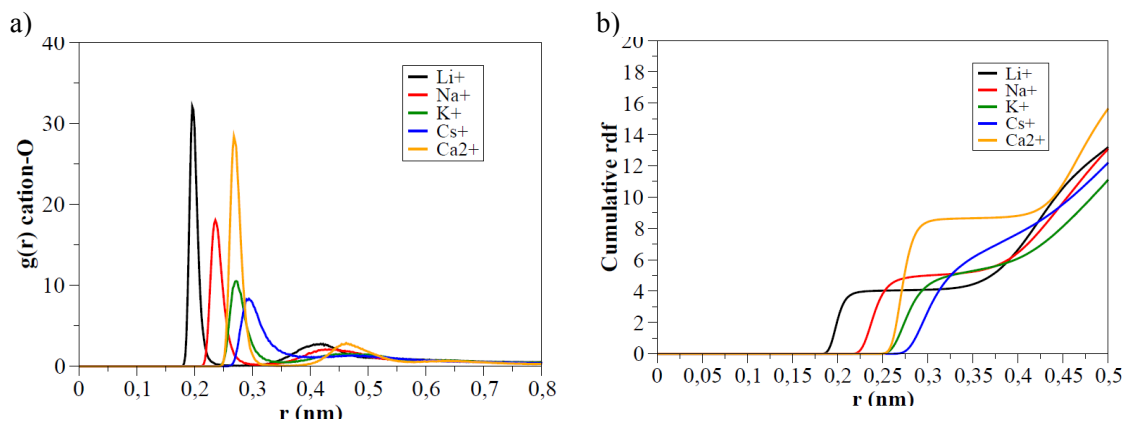


Fig. 11SI a) Radial distribution of the distance cation-O (water) inside the nanotube [$g_{\text{ion-oxygen}}(r)$] and b) cumulative distribution derived from the previous graphic.

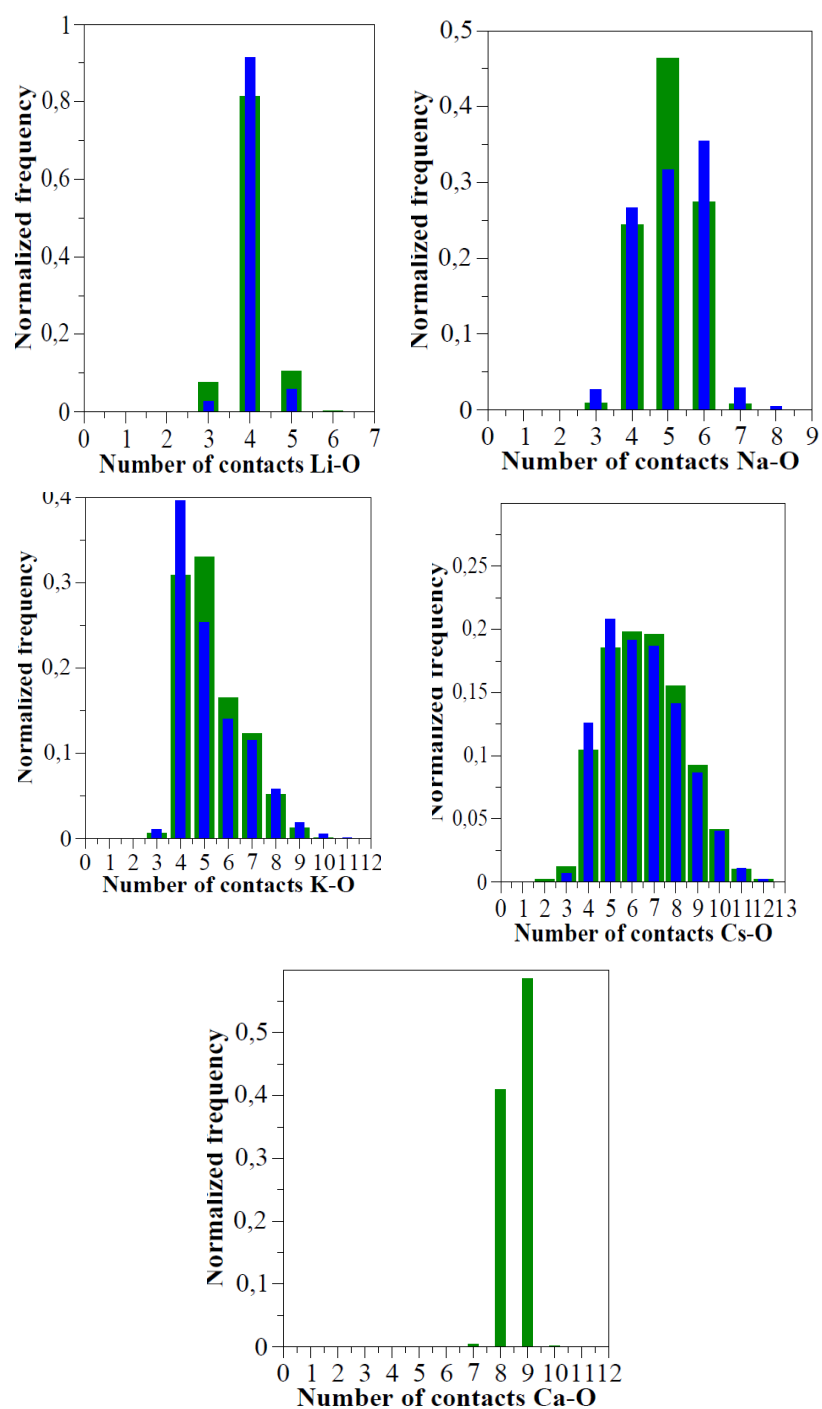


Fig. 12S Number of waters coordinated to the cations inside the nanotube, calculated from the contacts of the ions inside the channel at the distance of the radius of the first hydration shell. Each colour corresponds to an ion.

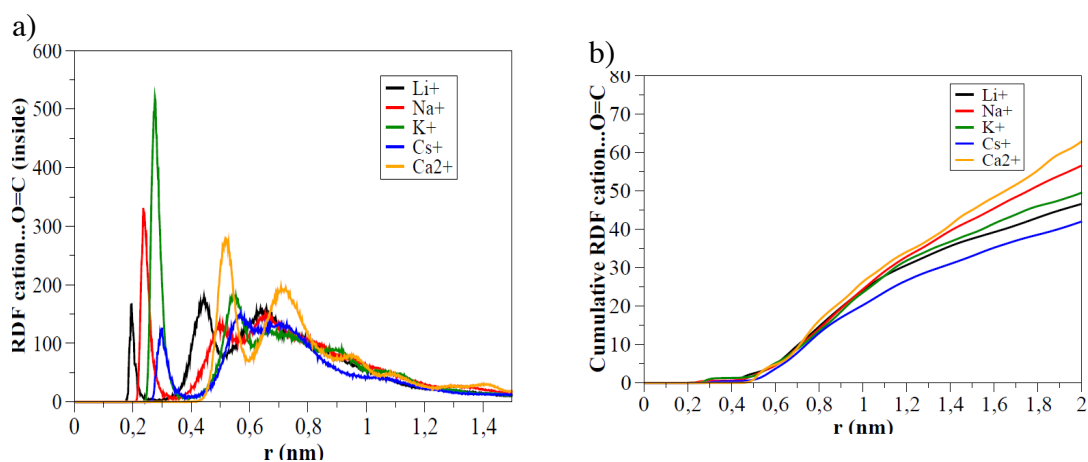


Fig. 13SI a) Radial distribution of the distance cation-O (carbonyl of the nanotube) inside the nanotube [$g_{\text{ion-oxygen_carbonyl}}(r)$] and b) cumulative distribution derived from the previous graphic.

The analyzed data reveals that the coordination distance cation-O (from the carbonyl group) increases with the size of alkaline cations from Li^+ to Cs^+ ($\text{K}^+ \sim \text{Cs}^+$), whereas it is maxima for the earth-alkaline Ca^{2+} , suggesting that no coordination to $\text{C}=\text{O}$ takes place in this last case, at least in a radius shorter than 5 Å from the center of the cation.

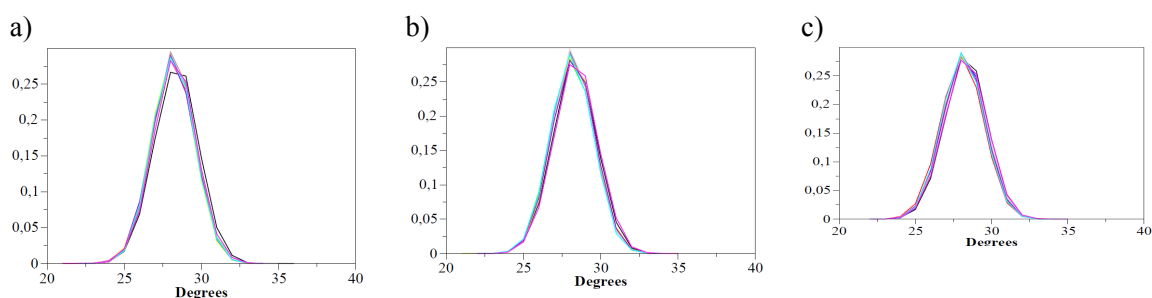


Fig. 14SI C(=O)N angle distributions along the MD simulations of 50 ns in a) pure water, b) in LiCl and c) in KCl. Each color represents a cyclic peptide (10 for all the cases).

The distributions of the angles formed by C(=O)N of each cyclic peptide were investigated and compared with the simulations in pure water, finding no much difference among both situations.

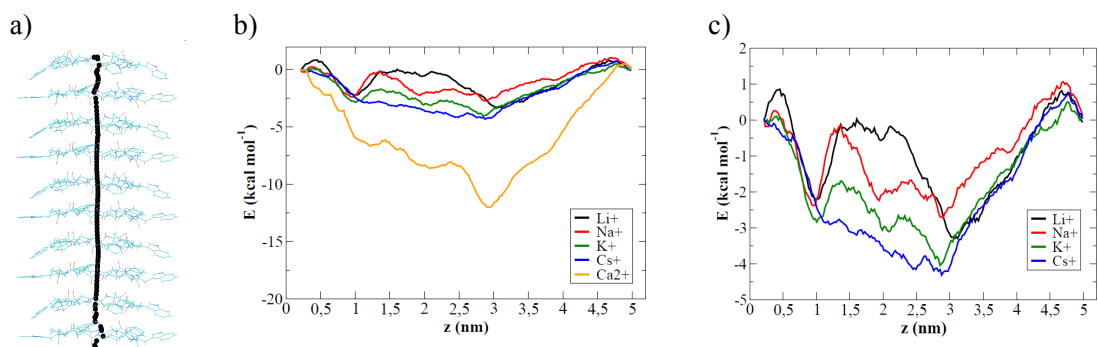


Fig. 15SI a) Starting positions of the cations inside the nanotube (after minimization). Each point corresponds to a cation and was simulated independently. b) Potentials of mean force (PMFs) for single ions as a function of position along the z-axis of the pore. c) Detail for the alkaline cations from the graphic before.²

² For all the alkaline cations except Cs⁺, especially Li⁺, the PMF shows a deep secondary minimum about two CPs from the mouth of the nanotube. This too is in keeping with the equilibrium MD results, in which all these ions, and particularly Li⁺, tended to remain stuck in these secondary minima (see Figures 3 and 6SI).

	60 mV		80 mV		120 mV	
	Conductance (pS)	Transport ($\times 10^7$ ions/s)	Conductance (pS)	Transport ($\times 10^7$ ions/s)	Conductance (pS)	Transport ($\times 10^7$ ions/s)
Cs^+ (CsCl)	43	1.63	38	1.88	34	2.56
K^+ (KCl)	43	1.63	36	1.81	31	2.31
Na^+ (NaCl)	40	1.50	34	1.69	28	2.06
Ratios of ion transport						
$\text{Cs}^+/\text{Na}^{+a}$		0.92		0.90		0.81
$\text{K}^+/\text{Na}^{+a}$		0.92		0.93		0.89
$\text{Cs}^+/\text{K}^{+a}$		1.00		0.96		0.90

Table S1. Ion transport and Conductivities for Na, K and Cs at several voltages and relationship between these data with their diffusion coefficient in water.

a) Estimated diffusion coefficient used, 2.6×10^{-5} cm²/s for Cs, 1.96×10^{-5} cm²/s for Cs, 1.33×10^{-5} cm²/s for Na, being the diffusion coefficients Cs/Na 0.65, K/Na 0.68 and Cs/K 0.95.

LiCl	61.49 (3.05)
NaCl	62.75 (2.67)
KCl	65.01 (2.66)
CsCl	65.88 (2.50)
CaCl₂	63.35 (2.62)

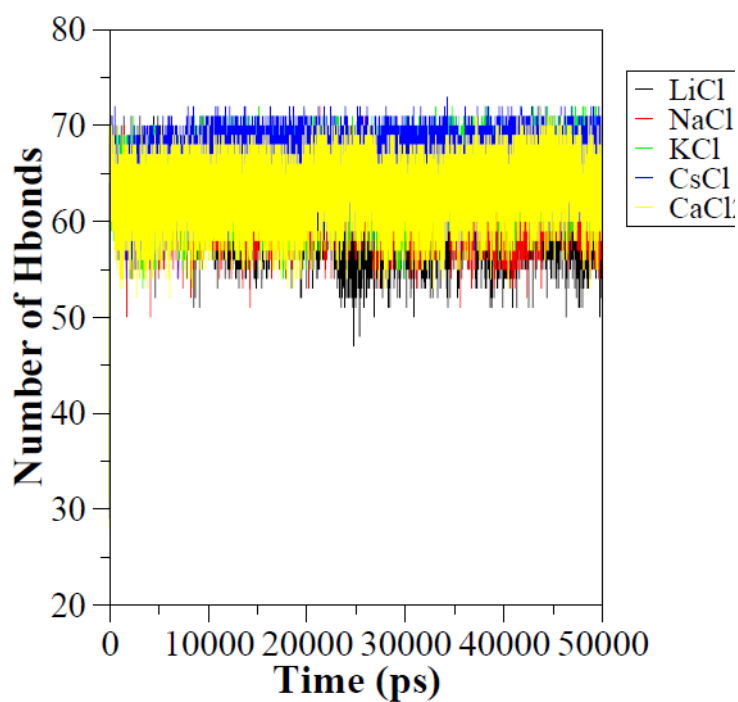


Table 2SI. Mean and standard deviation of the number of H-bonds between the cyclic peptides in different salt conditions. Graphical representation of the variation of these H-bonds along the trajectory (50 ns).

LiCl	73.44 (5.24)
NaCl	71.87 (5.67)
KCl	68.46 (4.92)
CsCl	69.19 (4.70)
CaCl₂	70.87 (5.19)

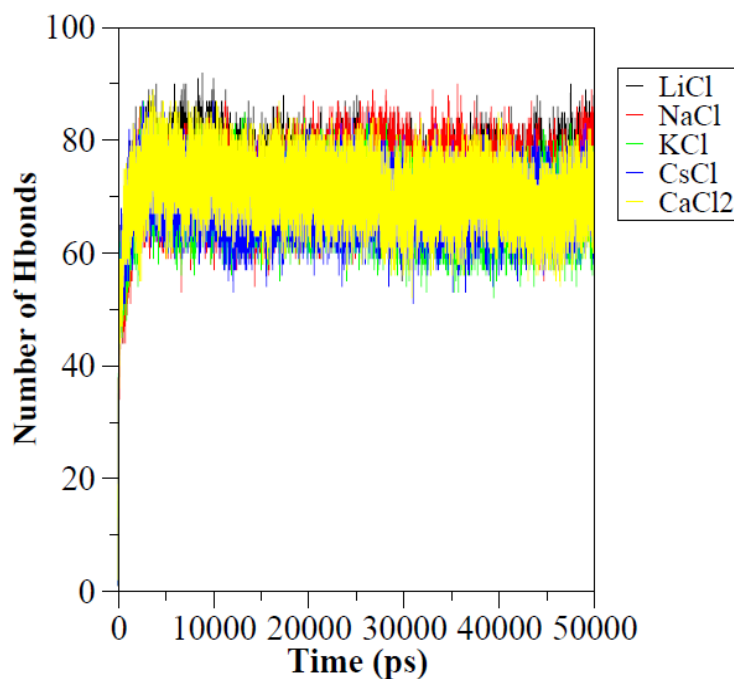


Table 3SI. Mean and standard deviation of the number of H-bonds between the cyclic peptides and the water in different salt conditions. Graphical representation of the variation of these H-bonds along the trajectory (50 ns).

	Cation	Anion (Cl)	Water
LiCl	2.48 (0.65)	0.011 (0.10)	90.60 (7.35)
NaCl	1.88 (0.57)	0.03 (0.2)	89.74 (7.34)
KCl	2.12 (0.55)	0.011 (0.011)	89.52 (7.83)
CsCl	2.14 (0.49)	0.0051 (0.071)	89.09 (6.84)
CaCl₂	1.09 (0.31)	0.037 (0.19)	90.83 (7.24)

Table 4SI. Mean and standard deviation of the number of ions and water inside the nanotube along the 50 ns of simulation in different salt concentrations.

	LiCl	NaCl	KCl	CsCl	CaCl₂
<i>Global</i>	0.00025 (0.00115)	0.0062 (0.0141)	0.0098 (0.0129)	0.0023 (0.0035)	0.0026 (0.0029)
<i>Only Z</i>	0.0008 (0.0033)	0.015 (0.043)	0.029 (0.040)	0.0072 (0.0115)	0.0077 (0.0085)

Table 5SI. Diffusion coefficients (mean and standard deviations along 50 ns of simulation) for the different salt concentrations studied. Units in (1e-5 cm²/s). Upper coefficients are global while those down are given parallel to the nanopore axis. For comparison, values for diffusion in bulk solution are Na⁺ 1.2, Cl⁻ 1.8, K⁺ 1.8 and Ca⁺² 0.53 x 10⁻⁹ m²/s.³

	Cation	Anion	Water
LiCl	2	0	34
NaCl	0	0	-20
KCl	1	0	18
CsCl	0	0	2
CaCl₂	0	0	-5

³ S. Koneshan, J. C. Rasaiah, R. M. Lynden-Bell, S. H. Lee, *J. Phys. Chem. B* **1998**, *102*, 4193-4204.

Table 6SI. Cumulative flux for ions and water across the nanotubes under the presence of an electric field (100 mV).

	Cation	Anion	Water
LiCl	2.25 (0.75)	0.0055 (0.074)	90.98 (6.31)
NaCl	1.91 (0.58)	0.0062 (0.078)	89.76 (7.71)
KCl	2.08 (0.59)	0.014 (0.012)	89.63 (7.08)
CsCl	2.08 (0.60)	0.014 (0.012)	89.62 (7.08)
CaCl₂	1.42 (0.64)	0.0054 (0.073)	90.14 (9.62)

Table 7SI. Mean and standard deviation of the number of ions and water inside the nanotube along the 50 ns of simulation in different salt concentrations, using an external electric field of 100 mV.

Materials and Methods.

General. 1-[bis(dimethylamino)methylene]-1*H*-benzotriazolium hexafluorophosphate 3-oxide (HBTU), 1-[bis(dimethylamino)methylene]-1*H*-benzotriazolium tetrafluoroborate 3-oxide (TBTU),⁴ alpha-aminoacids were purchased from Novabiochem or Advanced ChemTech. All reagents and solvents were used as received unless otherwise noted. ¹H NMR spectra were recorded on Varian Inova 400 MHz spectrometers. Chemical shifts (δ) were reported in parts per million (ppm) relative to tetramethylsilane (δ = 0.00 ppm) or by the deuterium solvent. ¹H NMR splitting patterns are designated as singlet (s), doublet (d), triplet (t), or quartet (q). All first-order splitting patterns were assigned on the basis of the appearance of the multiplet. Splitting patterns that could not be easily interpreted are designated as multiplet (m) or broad (br). Matrix-Assisted Laser Desorption/Ionization Time of Flight (MALDI-TOF) mass spectrometry was performed on a Bruker Autoflex mass spectrometer. Column chromatography was performed on EM Science silica gel 60 (230–400 mesh). Solvent mixtures for chromatography are re-reported as v/v ratios. CH₂Cl₂ and DIEA to be used as reaction solvents were distilled from CaH₂ over argon immediately prior to use.

(1*R*,3*S*)-N-Fmoc-3-aminocyclohexanecarboxylic acid (L-Fmoc-N-γ-Ach-OH). A solution of *L*-Boc-γ-MeN-Ach-OH⁵ (0.50 g, 2.058 mmol) in TFA/CH₂Cl₂ (1:1) was stirred at room temperature for 10 min. After removal of the solvent, the residue was dried under high vacuum for 2 h and then dissolved in dioxane/H₂O (1:1, 24 mL) and added Fmoc-Cl (0.692 g, 2.675 mmol). After 15 min, Na₂CO₃ (0.654 g, 6.174 mmol) was added and the mixture was stirred at room temperature for 4 h. The resulting solution was acidified at pH 2 and extracted with CH₂Cl₂ (3 x 20 mL). The combined organic layers were dried (Na₂SO₄), filtered, concentrated under reduced pressure, and the crude material was purified by flash chromatography (0-5% MeOH/CH₂Cl₂) to give *L*-Fmoc-N-γ-Ach-OH as a white solid [0.524 g, 70%; *R*_f 0.90 (10% MeOH en CH₂Cl₂), Fp 187-189 °C]. ¹H RMN (CDCl₃, 400 MHz, δ): 7.76 (d, *J* = 7.5 Hz, 2 H, Ar), 7.58 (d, *J* = 7.5 Hz, 2 H, Ar), 7.40 (t, *J* = 7.3 Hz, 2 H, Ar), 7.31 (t, *J* = 7.4 Hz, 2 H, Ar), 4.67 (d, *J* = 7.2 Hz, 1 H, NH), 4.40 (brs, 2 H, CH₂Fm), 4.22 (brs, 1 H, Fm), 3.54 (m, 1 H, H_γ), 2.46 (m, 1 H, H_α). ¹³C RMN (CDCl₃, 101 MHz, δ): 178.8 (C=O), 155.6 (C=O), 143.9 (C, Ar), 141.3 (C, Ar), 127.7 (CH, Ar), 127.0 (CH, Ar), 125.0 (CH, Ar), 120.0 (CH, Ar), 66.5 (CH₂), 49.3 (CH), 47.3 (CH), 41.7 (CH), 35.2 (CH₂), 32.6 (CH₂), 28.0 (CH₂), 24.1 (CH₂). **E.M.-FAB**

⁴ L. A. Carpino, H. Imazumi, A. El-Faham, F. J. Ferrer, C. Zhang, Y. Lee, B. M. Foxman, P. Henklein, C. Hanay, C. Mügge, H. Wenschuh, J. Klose, M. Beyermann, M. Bienert, *Angew. Chem.* **2002**, *114*, 457-461; *Angew. Chem., Int. Ed.* **2002**, *41*, 441-445.

⁵ a) M. Amorín, L. Castedo, J. R. Granja, *J. Am. Chem. Soc.* **2003**, *125*, 2844-2845; b) R. J. Brea, M. Amorín, L. Castedo, J. R. Granja, *Angew. Chem.* **2005**, *117*, 5856-5859; *Angew. Chem. Int. Ed.* **2005**, *44*, 5710-5713; c) C. Reiriz, R. J. Brea, R. Arranz, J. L. Carrascosa, A. Garibotti, B. Manning, J. M. Valpuesta, R. Eritja, L. Castedo, R. J. Granja, *J. Am. Chem. Soc.* **2009**, *131*, 11335-11337.

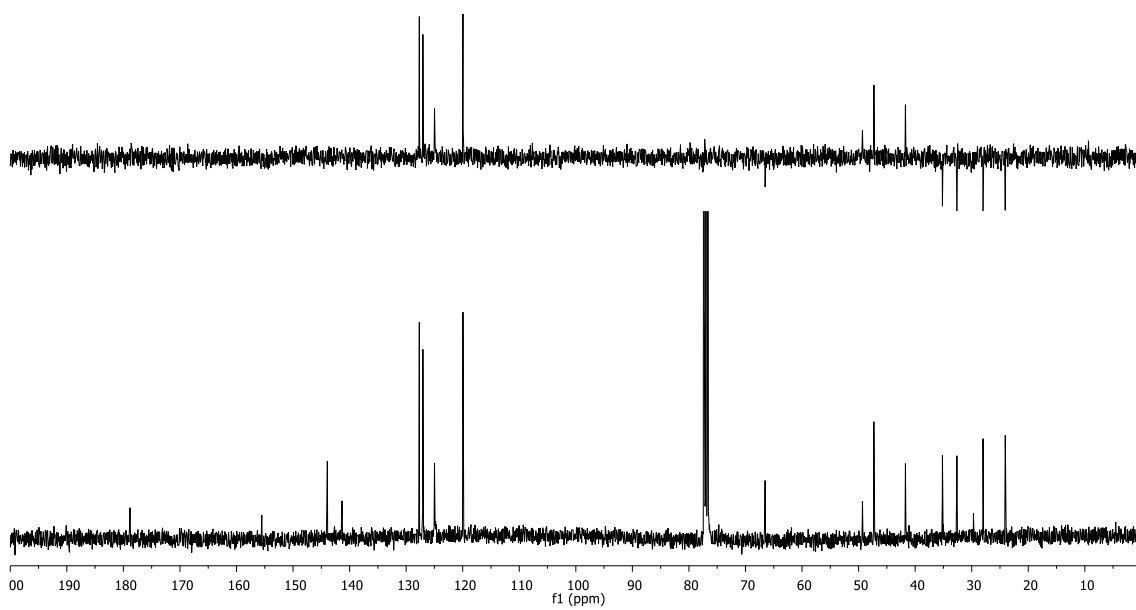
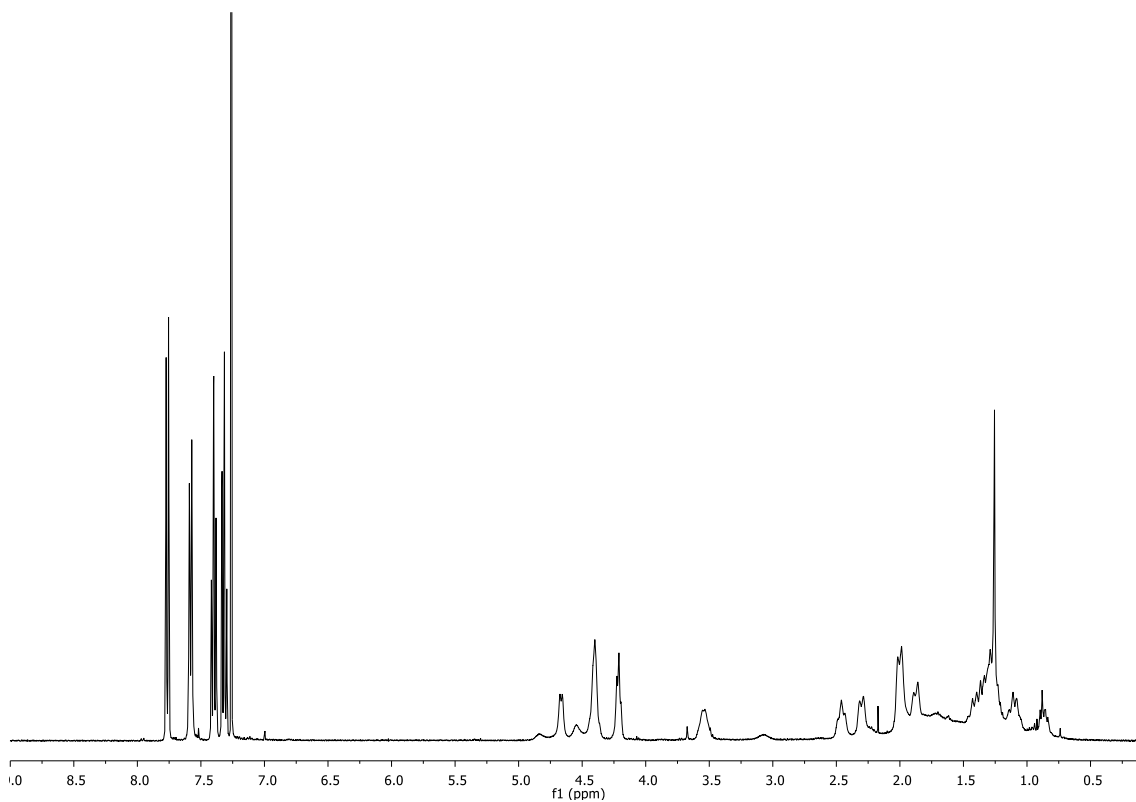
[*m/z* (%): 368.1 (MH⁺, 12.4). **E.M. (FAB⁺)** [*m/z* (%): 366 ([MH]⁺, 62), 197 ([Fm-OH]⁺, 100). **E.M.-HR [MH]⁺ calculated for C₂₂H₂₄NO₄**: 366.17053, **found**: 366.17069.

(1*S*,3*R*)-N-Fmoc-3-aminocyclohexanecarboxylic acid (D-Fmoc-N-γ-Ach-OH). This compound was obtained following the procedure described for **L-Fmoc-N-γ-Ach-OH**, starting from **D-Boc-N-γ-Ach-OH** (0.75 g, 3.087 mmol).

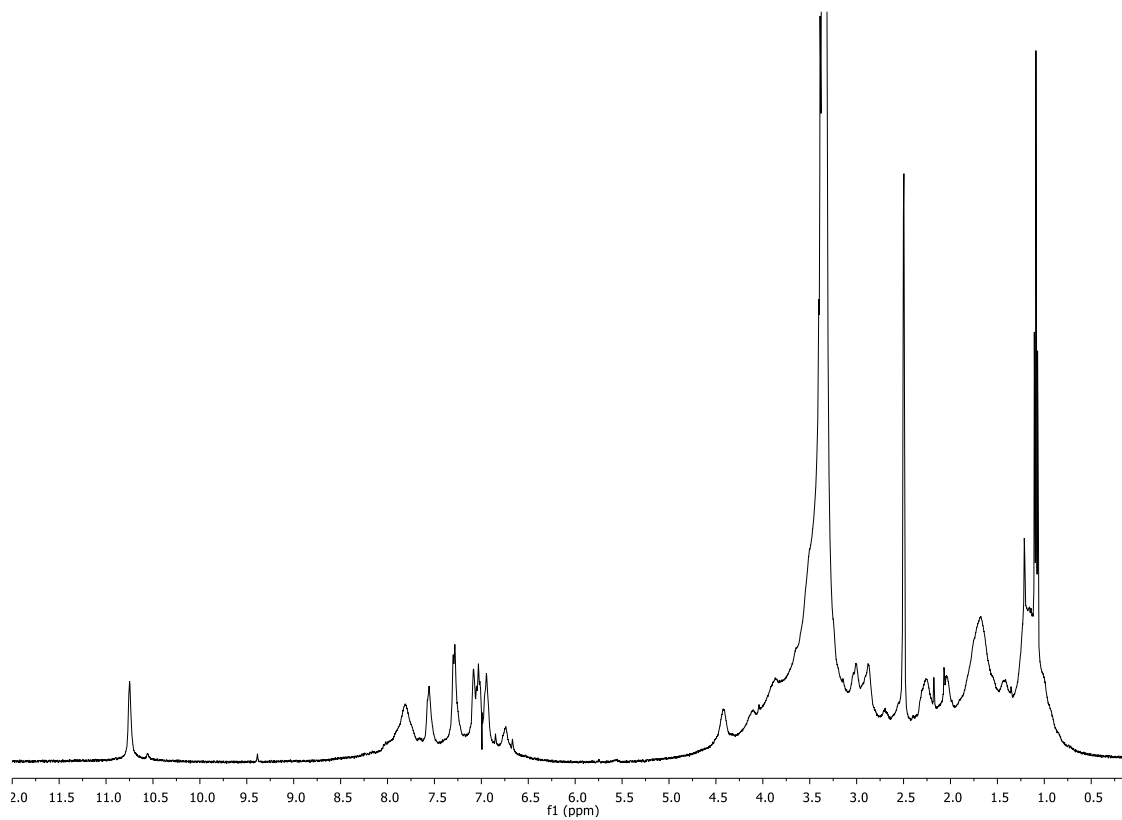
Solid-Phase Peptide Synthesis (SPPS). Peptides *c*-[(*D*-γ-Ach-*L*-Trp)₂-*D*-γ-Ach-*L*-Gln-] (**CP1**), *c*-[(*D*-γ-Ach-*L*-Trp)₃-*D*-γ-Ach-*L*-Gln-] (**CP2**), *c*-[*D*-Trp-*L*-γ-Ach-*D*-Trp-*L*-Leu-*D*-Trp-*L*-γ-Ach-*D*-Trp-*L*-Gln-] (**CP3**) were synthesized by manual fluorenylmethyloxycarbonyl (Fmoc) solid-phase peptide synthesis from peptide synthesis from *L*-Fmoc-Glu(Rink Resin)-OAll. Typically, *L*-Fmoc-Glu(Rink Resin)-OAll (0.47 mmol/g) was placed in a peptide synthesis vessel and swelled with CH₂Cl₂ (3x 1 min) and DMF (3 x 1 min). Coupling cycle consisted of, a) Fmoc group deprotection (20% piperidine in DMF, 2 x 15 min), b) DMF wash (6 x 1 min), c) amino acid coupling [for α-amino acids: *L*-Fmoc-α-Aa-OH (4.0 eq.), HBTU (3.95 eq.), and DIEA (16 eq.), while for γ-amino acids: *D*-Fmoc-γ-Ach-OH (2.0 eq.), HBTU (1.97 eq.), and DIEA (8.0 eq.) dissolved in DMF (final Aa concentration 0.1 M)] and the mixtures were shaken for 1 h, and d) DMF washes (6 x 1 min). After lineal synthesis on solid phase was completed, the C-terminal protecting group (All) was removed with *in situ* generated Pd(PPh₃)₄ by mixing PPh₃ (1.25 eq.), N-methylmorpholine (10.0 eq.), phenylsilane (10.0 eq.) and Pd(OAc)₂ (0.25 eq) in CH₂Cl₂ under Ar and the resulting suspension was stirred for 15 min after a yellow solution is form. This mixture was added to the resin and the mixture was stirred under Ar at room temperature for 12 h. After removing the solution, the resin was washed with CH₂Cl₂ (4 x 1 min), 2% DIEA in DMF (4 x 1 min), 0.5% sodium diethyldithiocarbamate in DMF (4 x 1 min), and DMF (4 x 1 min). The N-terminal protecting group (Fmoc) was removed with piperidine in DMF (20%, 2 x 15 min), and then washed with DMF (6 x 1 min), 5% DIEA in DMF (6 x 1 min), 5% solution of 0.8 M of LiCl in TFA, and again DMF (6 x 1 min). The peptide was cyclized by adding TBTU (3.0 eq.) and DIEA (8.0 eq.) in DMF (coupling reagent concentration 0.5 M), followed by stirring for 24 h. After filtration and washing with DMF (4 x 1 min), CH₂Cl₂ (4 x 1 min), MeOH (2 x 1 min), CH₂Cl₂ (1 x 1 min) y ethyl ether (4 x 1 min), the resin was dried under high vacuum. Peptides were generally deprotected and cleaved from the resin by standard TFA cleavage procedure (TFA/H₂O/TIS (95:2.5:2.5, 1 h at rt). After filtration to remove the solid support, the solution was cooled down in an ice bath and the peptide was precipitated by addition of cold Et₂O, the precipitate was centrifuged and washed with Et₂O. The cyclic peptides were purified by dissolving it in DMF and precipitated out with ether and the solids were washes with acetonitrile and water (1:1). **CP1**: ¹H RMN (DMSO, 400 MHz, δ): 10.75 (s, 2 H, NH), 7.81 (br, 3 H, NH), 7.56 (brd, *J* = 6.5 Hz, 2 H, Ar), 7.29 (d, *J* = 6.6 Hz, 2 H, Ar), 7.03 (m, 2 H, Ar), 7.01 (m, 2 H, Ar), 6.95 (brs, 2 H, Ar), 6.85 (brs, 1 H, NHε), 4.42 (brs, 2

H, H α). **MALDI-TOF** [m/z (%): 898 ([MNa]⁺, 100); 914 ([MK]⁺, 21). **MALDI-TOF-HR** [MNa]⁺ calculated for C₄₈H₆₁N₉NaO₇: 898.4586, found: 898.4570. **CP2**: ¹H RMN (DMSO, 400 MHz, δ): 10.74 (s, 3 H, NH), 7.82 (brs, 4 H, NH), 7.56 (d, J = 8.5 Hz, 3 H, Ar), 7.28 (d, J = 6.9 Hz, 3H, Ar), 7.08 (br, 3 H, Ar), 7.06-6.90 (m, 6 H, Ar), 6.74 (br, 1 H, NH ϵ), 4.42 (brs, 3 H, H α). **MALDI-TOF** [m/z (%): 1210 ([MNa]⁺, 100); 1226 ([MK]⁺, 20). **MALDI-TOF-HR** [MNa]⁺ calculated for C₆₆H₈₂N₁₂NaO₉: 1209.6220, found: 1209.6279. **CP3**: ¹H RMN (DMSO, 400 MHz, δ): 10.74 (m, 4 H, NH), 8.5-7.50 (overlapped m, 4 H, NH), 7.95 (brs, 4 H, Ar), 7.28 (d, J = 7.9 Hz, 4 H, Ar), 7.14-6.93 (m, 12H, Ar), 6.70 (brs, 1 H, NH ϵ Gln). **MALDI-TOF** [m/z (%): 1259 ([MNa]⁺, 100); 1275 ([MK]⁺, 36). **MALDI-TOF-HR** [MNa]⁺ calculated for C₆₉H₈₁N₁₃NaO₉: 1258.6172, found: 1258.6164.

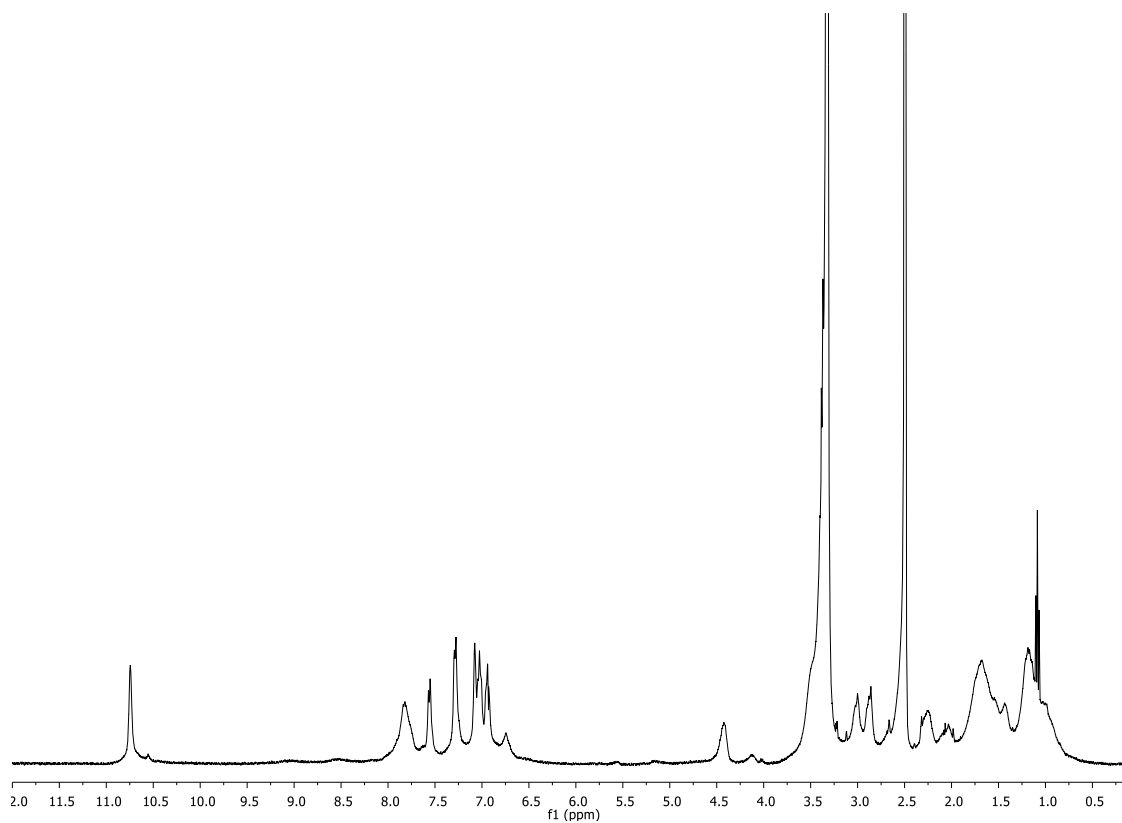
(1*R*,3*S*)-N-Fmoc-3-aminocyclohexanecarboxylic acid (L-Fmoc-N- γ -Ach-OH). NMR data:



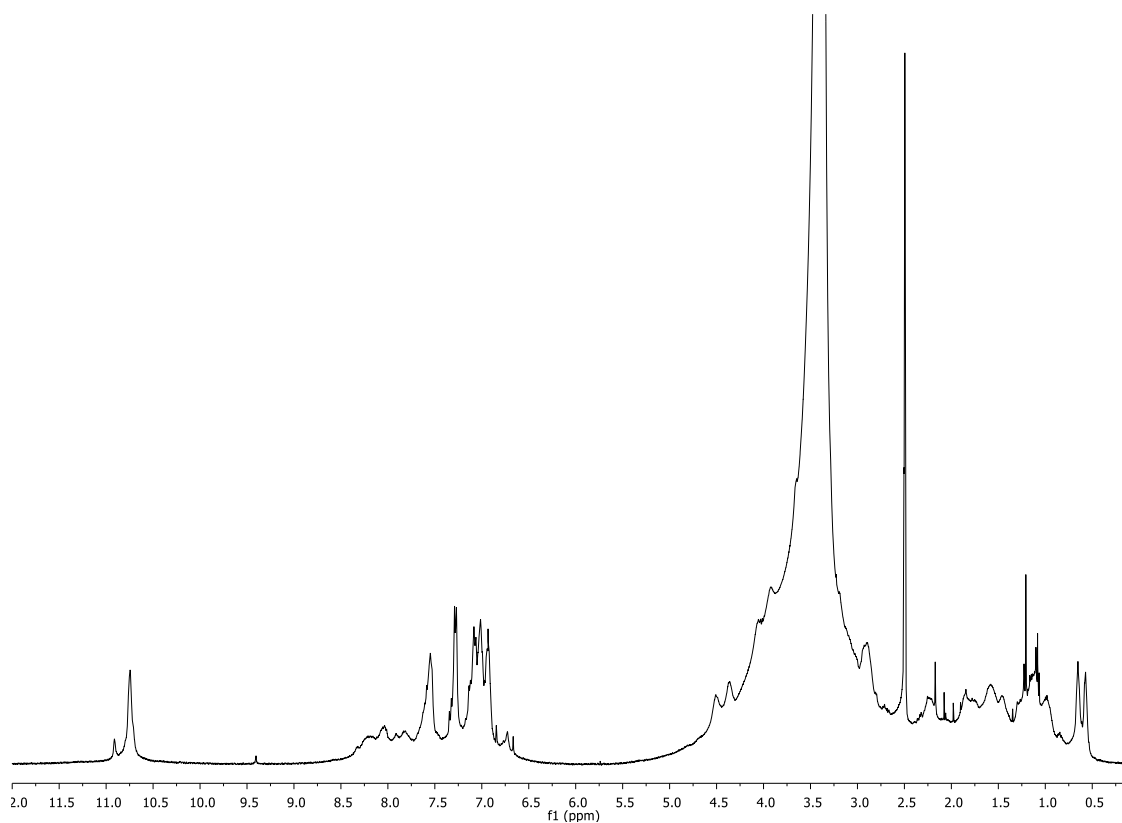
CP1. ^1H NMR:



CP2. ^1H NMR:



CP3. ^1H NMR:

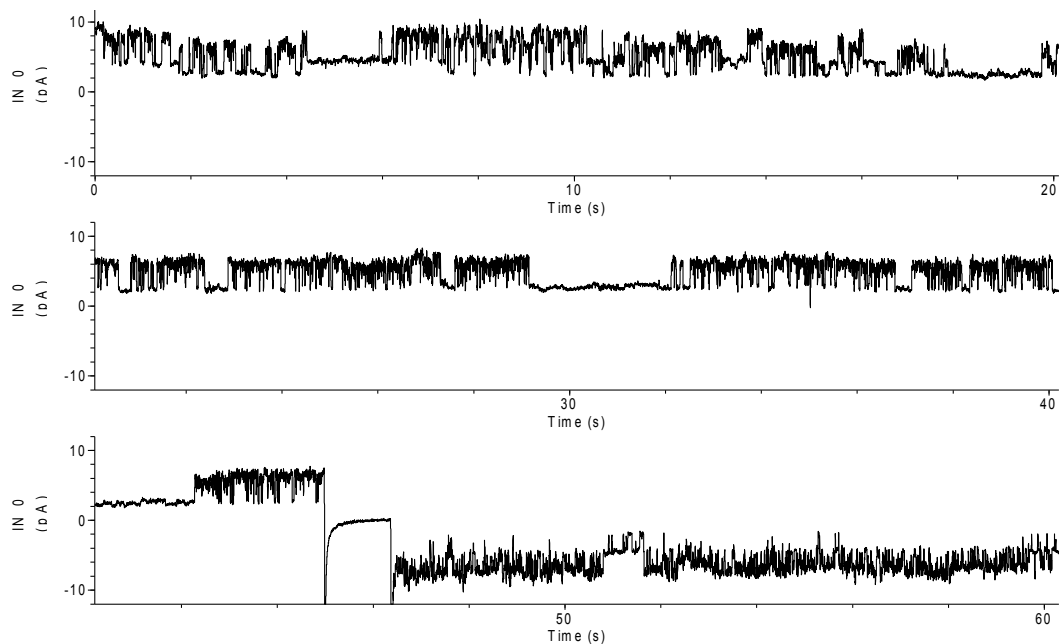


Bilayer Recording. Bilayers were formed using either 1,2-diphytanoyl-*sn*-glycero-3-phosphocholine, a 3:1 mixture of 1-palmitoyl-2-oleoyl-*sn*-glycero-3-phosphoethanolamine (POPE): 1-palmitoyl-2-oleoyl-*sn*-glycero-3-phospho-(1'-*rac*-glycerol) (sodium salt) (POPG) or 1,2-diphytanoyl-*sn*-glycero-3-phosphocholine, following the method described by Montal and Muller⁶ on a 80-100 μm orifice in a 25 mm Teflon film (Goodfellow Corporation, Malvern, PA, USA) separating the two chambers, *cis* and *trans*, of a PTFE planar bilayer apparatus. Each chamber contained 0.5 mL of 0.5 M of chloride salt (LiCl, NaCl, KCl, CsCl or CaCl₂), 10 mM MOPS titrated to pH 7.5 with KOH except for NaCl studies in which NaOH was used. The electrodes were Ag/AgCl in 1.5% agarose containing 3 M KCl, or the electrodes were Ag/AgCl pellets connected to a silver wire (E206, In Vivo Metric, Healdsburg, CA, USA). The *cis* chamber was at virtual ground. A positive potential indicates a higher potential in the *trans* chamber, and a positive current is the one in which cations flow from the *trans* to the *cis* chamber. Ion channel forming cyclic peptides were dissolved either in 10% DMSO in methanol for the 0.1 mM CP concentration or in 1% DMSO in methanol for the solutions with peptide concentration 0.01 mM. 1 to 2 μL of the cyclic peptide stock solution were added to each chamber (final concentration in the chamber: 0.2 to 0.02 mM).

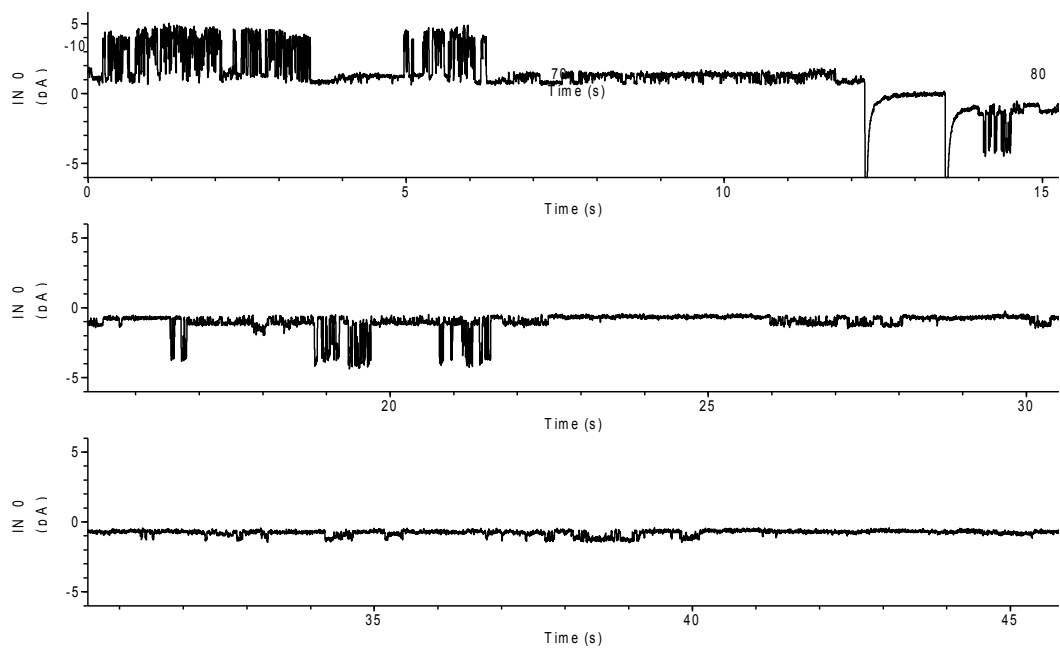
Data collection, processing and analysis. Raw ion current recording was acquired at 1 kHz or higher using a 3900A Integration Match Clamp (Dagan Corporation, MN, USA) that was used *via* a Digidata 1200 A/D (Axons instruments) converter or Axopatch 200B *via* a Digidata 1322 D/A, while data collection was done by the Clampex 9 or 10 software. Data processing and analysis was carried out with Clampfit 9 or Clampfit 10. All Axons instruments and software are products of Molecular Devices (Sunnyvale, CA).

Conductance values were obtained automatically by programming the applied transmembrane potentials or manually by extracting the data from all point histograms or directly from single channel activity traces.

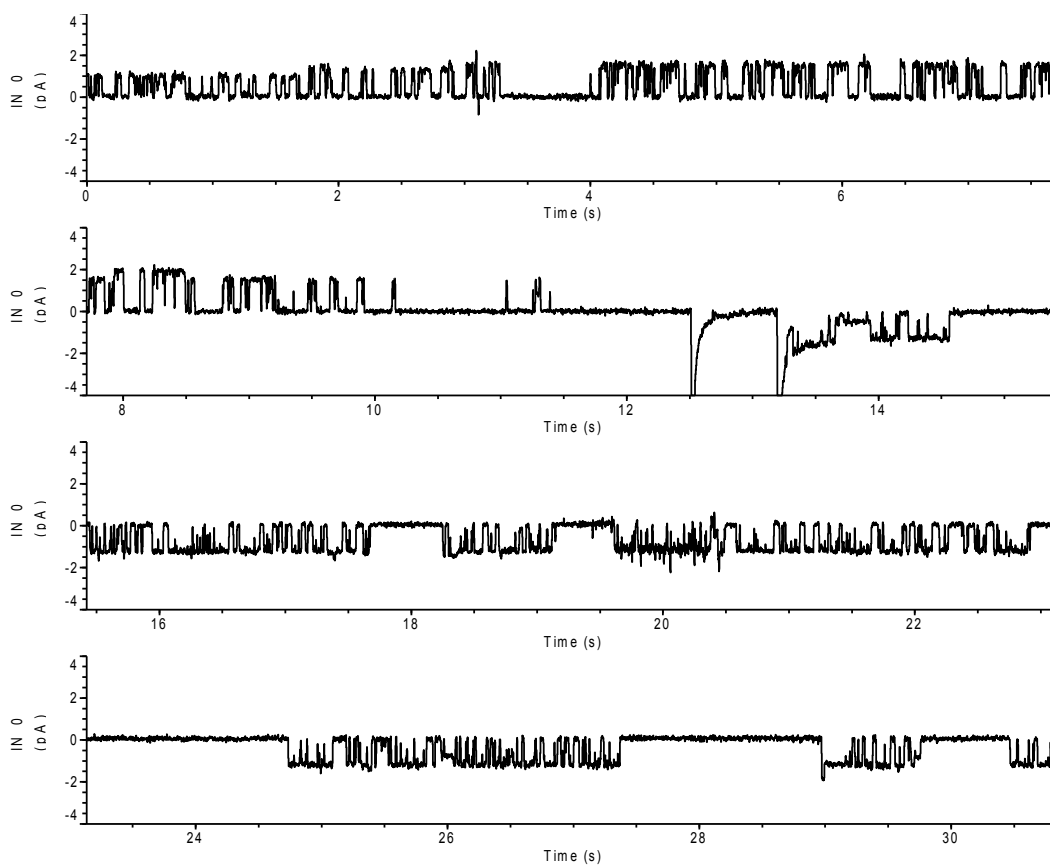
⁶ M. Montal, P. Mueller, *Proc. Natl. Acad. Sci. U.S.A.* **1972**, *69*, 3561-3566.



60 seconds ion channels activity recording for CsCl 0.5 mM (10 mM MOPS. DPPC) at +80mV and -80 mV. two levels at 1.8 and 3.0 pA are observed.



46 seconds ion channels activity recording for KCl 0.5 mM (10 mM MOPS. DPPC) at +60 mV and -60 mV. three levels at 0.5, 2.6 and 3.1 pA are observed, corresponding the last one to both channels open at the same time.



31 second ion channels activity recording for NaCl 0.5 mM (10 mM MOPS, DPPC) at +100mV and -100 mV. Three levels at 1.1, 1.5 and 1.8 pA are observed.

Theoretical studies:

Methods:

The starting geometries of the cyclic peptides investigated in this work were constructed from X-ray crystallographic data of related compounds: *c*-[(*D*-Phe-*L*-^{Me}N- γ -Ach)₄].⁷ From the structures of the dimers, the N-methyl groups were removed and changed by N-H and the dimers were then replicated five times along the axis perpendicular to the CP planes, by a distance equal to that measured between the two original CP units. Therefore, the resulting SCPNs are composed by ten CPs units.

Concerning the atoms of the SCPN, RESP/6-31G(d) charges were derived as in the original AMBER force-field development, while van der Waals parameters were taken from the GAFF force-field⁸ using standard Lorenz-Bertelot combination rules. Bonded terms were taken as those of standard peptides. We used the water (SPC/E) / ion combination parameters published by Joung et al.⁹ implemented in AMBER10 to prevent crystallization previously reported at high concentrations with other parameter sets.¹⁰ The GAFF force field was used for DOPC lipids, employed also in previous studies¹¹ from which we obtained a pre-equilibrated membrane for subsequent replication. The bilayer was replicated three times in x and y directions (or only twice in the case of the PMF calculations), and after SCPN insertion, the complete system was solvated. Water in the hydrophobic region of the tails and also inside of the SCPN was removed, so that in the first step of the simulation the channel was completely dry. The resultant system was ionized using different salt concentrations (LiCl, NaCl, KCl, CsCl and CaCl₂ 0.5M, respectively). The initial size of the unit cell was equal to 15.1 x 15.2 x 6.9 nm³ and contained ~555 lipids, ~476 cations and ~18000 water molecules.

The equilibrium simulations were performed with the GROMACS 4.0¹² molecular dynamics program. All the systems were partially optimized, thermalized, and equilibrated, followed by unrestrained simulations for 50 ns (time step=2 fs) for each one of the systems studied. The constant pressure and temperature canonical ensemble was employed with the pressure of 1 bar controlled using a semi-isotropic Parrinello-Rahman barostat,¹³ and the temperature of 300K imposed by a V-rescale thermostat (Temperature coupling using velocity rescaling with a

⁷ M. Amarin, L. Castedo, J. R. Granja, *Chem. Eur. J.* **2005**, *11*, 6543-6551.

⁸ a) J. Wang, W. Wang, P. A. Kollman, D. A. Case, *J. Mol. Graphics Modell.* **2006**, *25*, 247260. b) J. Wang, R. M. Wolf, J. W. Caldwell, P. A. Kollman, D. A. Case, *J. Comput. Chem.* **2004**, *25*, 1157-1174.

⁹ I. S. Joung, T. E. Cheatham, *J Phys Chem B* **2008**, *112*, 9020-9041.

¹⁰ D. A. Case, T. A. Darden, T. E. Cheatham, C. L. Simmerling, J. Wang, R. E. Duke, R. Luo, M. Crowley, R. C. Walker, W. Zhang, K. M. Merz, B. Wang, S. Hayik, A. Roitberg, G. Seabra, I. Kilossváry, K. F. Wong, F. Paesani, J. Vanicek, X. Wu, S. R. Brozell, T. Steinbrecher, H. Gohlke, L. Yang, C. Tan, J. Mongan, V. Hornak, G. Cui, D. H. Mathews, M. G. Seetin, C. Sagui, V. Babin, P. A. Kollman, (2008), AMBER 10, University of California, San Francisco.

¹¹ S. W. I. Siu, R. Vacha, P. Jungwirth, R. A. Böckmann, *J. Chem. Phys.* **2008**, *128*, 125103. The structure of the membrane was downloaded from <http://www.bioinf.uni-sb.de/RB>

¹² B. Hess, C. Kutzner, D. van der Spoel, E. Lindahl, *J. Chem. Theory Comput.* **2008**, *4*, 435-447.

¹³ M. Parrinello, A. Rahman, *J Appl Phys* **1981**, *52*, 7182-7190.

stochastic term).¹⁴ The LINCS¹⁵ algorithm was employed to remove the bond vibrations. The Particle Mesh Ewald method¹⁶ coupled to periodic boundary conditions was used to treat the long-range electrostatics using a direct-space cutoff of 1.0 nm and a grid spacing of 0.12 nm. Van der Waals interactions were computed using PBC coupled to a spherical *cutoff* of 1.0 nm.

The potential of mean force (PMF) of the specific ion moving through the investigated nanotubes was calculated using umbrella sampling. The 1D reaction pathway corresponds to the distance along the *z* axis of the SCPN. For umbrella sampling, the particle of interest was harmonically restrained to subsequent positions on the channel axis (with typical values of the restraining force constant 1000 kJ mol⁻¹ nm⁻²) in 100 windows of with $\Delta z = 0.05$ nm. This restricted its movement to the *xy*-plane while still allowing diffusion into adjacent windows. Each window was initially minimized. One MD simulation of length 1 ns was carried out for each of the 100 windows. The 100 biased distributions of *z* positions of the test particle were recombined and unbiased with the Weighted Histogram Analysis Method (WHAM).¹⁷ The first 0.6 ns of each window run were discarded as equilibration time, leaving a total of 0.4 ns per window.

Data were analyzed using GROMACS and locally written code. Molecular graphic images were prepared using visual molecular dynamics (VMD).¹⁸ The analysis of ions and waters inside use carried out using Gridcount.¹⁹

¹⁴ G. Bussi, D. Donadio, M. Parrinello, *J. Chem. Phys.* **2007**, *126*, 014101.

¹⁵ B. Hess, H. Bekker, H. J. C. Berendsen, J. G. E. M. Fraaije, *J. Comput. Chem.* **1997**, *18*, 1463-1472.

¹⁶ U. Essman, L. Perera, M. Berkowitz, T. Darden, H. Lee, L. Pedersen, *J. Chem. Phys.* **1995**, *103*, 8577-8593.

¹⁷ a) S. Kumar, J. M. Rosenberg, D. Bouzida, R. H. Swendsen, P. A. Kollman, *J. Comput. Chem.* **1995**, *16*, 1339-1350. b) A. Grossfield, (accessed August 2008) An implementation of WHAM: the weighted histogram analysis method, <http://membrane.urmc.rochester.edu/Software/WHAM/WHAM.html>. c) Sm Kumar, D. Bouzida, R. H. Swendsen, P. A. Kollman, J. M. Rosenberg, *J. Comp. Chem.* **2002**, *13*, 1011-1021.

¹⁸ W. Humphrey, A. Dalke, K. Schulten, *K. J Mol Graphics* **1996**, *14*, 33-38.

¹⁹ O. Beckstein, M. S. P. Sansom, *Proc. Natl. Acad. Sci. U.S.A.* **2003**, *100*, 7063-7068.